Joint Pathology Center
Veterinary Pathology Services

WEDNESDAY SLIDE CONFERENCE 2025-2026

Conference #20 25 March 2026

CASE I:

Signalment:

Adult, castrated male, wild donkey (*Equus africanus asinus*)

History:

Seven wild donkeys died over the course of a week following a history of respiratory signs. Two of the donkeys were submitted for postmortem examination and diagnostic workup. Tissues from one of these animals are included here.

Gross Pathology:

The lungs are diffusely swollen with a lobular pattern. On the cut surface, red areas of pulmonary consolidation are seen in a lobular pattern, separated by unaffected lung lobules. Moderate amounts of thick tan exudate are noted in the airways. The trachea contains moderate amounts of stable foam. The tracheobronchial lymph nodes are enlarged.

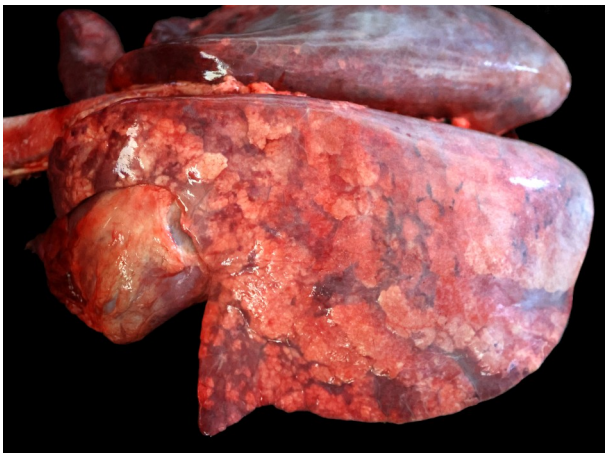

Figure 1-1. Lung, donkey: The lungs fail to collapse and are diffusely swollen with a lobular pattern (*Photo courtesy of*: California Animal Health and Food Safety Laboratory System (CAHFS), San Bernardino Laboratory, https://cahfs.vetmed.ucdavis.edu/locations/san-bernardino-lab)

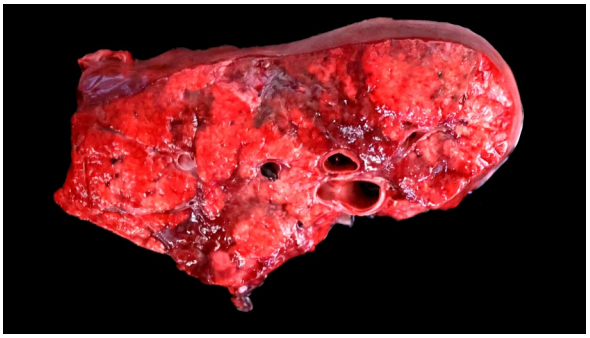

Figure 1-2. Lung, donkey. On the cut surface, there is pulmonary consolidation in a lobular pattern separated by unaffected or overinflated lung lobules. (*Photo courtesy of*: California Animal Health and Food Safety Laboratory System (CAHFS), San Bernardino Laboratory, https://cahfs.vetmed.ucdavis.edu/locations/san-bernardino-lab) .

Laboratory Results:

Virology: Influenza A virus was detected in nasal and bronchial swabs, as well as in the lung. Whole genome sequencing successfully recovered 16% (2.1 kb) of the entire equine influenza virus genome. The strain was highly similar (>99.7% nucleotide identity) to multiple strains (H3N8) from the United States and Chile.

-Equine herpesvirus 1 and 4 (EHV-1 and EHV-4) were not detected by PCR.

-No viral particles were detected by virus isolation (nasal and bronchial swabs and lung).

Bacteriology: Mixed flora was isolated form the lung.

Electron microscopy: No viral particles were detected in the lung.

Contributor's Comment:

Equine influenza virus A (EIV) is an enveloped, single-segmented, negative-sense RNA virus belonging to the Orthomyxoviridae family and Influenza A genus.[8] In equids, two main subtypes have been described: H7N7 (extinct since 1979) and H3N8.[1] H3N8 infects and causes disease in horses, donkeys, dogs, pigs, and camels, and there is evidence that it occasionally infects humans.[7,14,15] Outbreaks of H3N8 in donkeys have been identified in several regions and countries, including the United States, Brazil, Chile, Europe, China, Senegal, Pakistan, Turkey, West and Central Africa, Egypt, and India.[1] Only a few countries such as New Zealand and Iceland are free of equine influenza.[3] H3N8 strains have been considered emerging in donkeys in Colorado, California, and China.[1,14] Outbreaks of H3N8 show

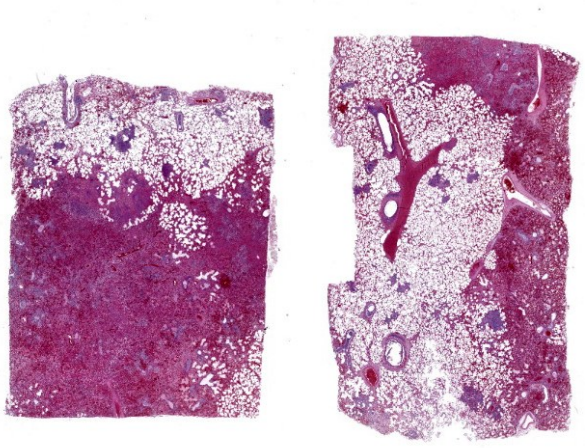

Figure 1-3. Lung, donkey: In the submitted sections of lung, over 50% of the pulmonary parenchyma is consolidated. (HE, 10X)

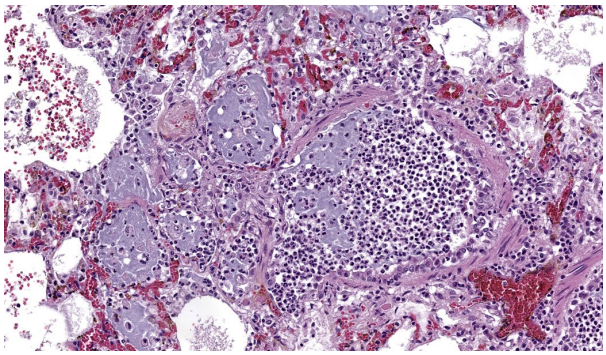

Figure 1-4. Lung, donkey: Throughout the section, airways are filled with large numbers of neutrophils, macrophages, mucin, and cellular debris. There is segmental necrosis and loss of airway epithelium. The inflammatory exudate extends into and fills adjacent alveoli.

no age predilection; morbidity is often high (81%) and mortality is low, although it can reach up to 20%, particularly in donkeys.[8,11,14] Donkeys are more susceptible to EIV infection compared to horses,[3,12] possibly due to a higher propensity for bacterial bronchopneumonia or recurrent coinfections with *Dictyocaulus arnfieldii*.[3]

EIV is extremely contagious and transmission occurs by direct contact with infected animals or fomites, as well as via aerosols. It can effectively travel through the air over distances of up to 1-2 km.[12] The incubation period ranges from 1 to 3 days.[12] EIV primarily infects respiratory tract epithelial cells through receptor-mediated endocytosis. The spike glycoprotein, HA, attaches to sialic acid receptors on the host cell surface.[10,12] Viral replication leads to epithelial cell death, mostly through apoptosis, and subsequent chemotaxis of immune cells, causing inflammation and reducing mucociliary clearance.[10]

Uncomplicated cases of EIV infection are typically mild and self-limiting. In equids, clinical signs include nasal serous or mucopurulent discharge, dry cough, pyrexia, loss of appetite, weakness, poor performance,

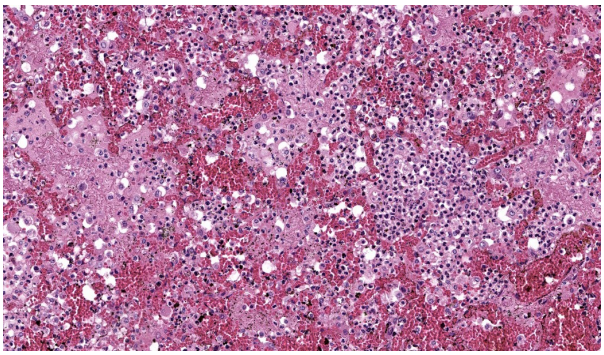

Figure 1-5. Lung, donkey: In inflamed areas, alveoli septa are filled with numerous neutrophils, alveolar macrophages, edema, hemorrhage, and polymerized fibrin. Alveolar septa are markedly congested with mild edema, increased numbers of circulating neutrophils, and occasional Type II pneumocyte hyperplasia.

and hyperemia of nasal and conjunctival mucosae.[9] Clinical signs are generally milder in horses and mules compared to donkeys.[12] Fatal cases may occur with complications from pulmonary bacterial infections such as those caused by *Streptococcus equi* subsp. *zooepidemicus*, *Streptococcus* spp., *Klebsiella pneumoniae*, and *Actinobacillus* spp.[5,6,11,14] Rare complications include myocarditis, chronic obstructive pulmonary diseases, and encephalitis.[9,12]

Typical pathological changes in equids with viral pneumonia include pulmonary consolidation in a lobular pattern separated by unaffected or overinflated lung lobules, or less commonly, a diffuse pattern of pneumonia.[1] EIV infections complicated by secondary bacterial infections are characterized by fibrinosuppurative exudate and pulmonary consolidation, mostly restricted to the cranioventral pulmonary lobes (bronchopneumonia).[1,12,13] Histologically, acute stages typically reveal rhinitis and tracheitis with epithelial necrosis and infiltrates of lymphocytes in the lamina propria. Subacute to chronic lesions consist of epithelial hyperplasia and squamous metaplasia.[6,11] Affected lungs exhibit bronchointerstitial pneumonia with hyaline membranes in the alveoli, type II pneumocyte hyperplasia, and necrotizing bronchitis/bronchiolitis. Secondary bacterial bronchopneumonia may also develop.[4,6,12]

Other viral upper respiratory infections such as Equine Herpesvirus 1 (EHV-1) and Equine Herpesvirus 4 (EHV-4) produce similar lesions and should be considered as differential diagnoses in donkeys.[2] Confirmation of the etiology in cases of EIV infection should involve fluorescent antibody testing (FAT), immunohistochemistry (IHC), virus isolation, molecular testing, and/or partial genetic and phylogenetic analysis of the virus.[10]

Contributing Institution:

California Animal Health and Food Safety Lab
105 W Central Ave, San Bernardino, CA 92408, USA.
https://cahfs.vetmed.ucdavis.edu/

JPC Morphologic Diagnosis:

Lung: Pneumonia, bronchointerstitial, necrotizing and fibrinosuppurative, acute, multifocal to coalescing, marked, with thrombosis, edema, and hyaline membranes.

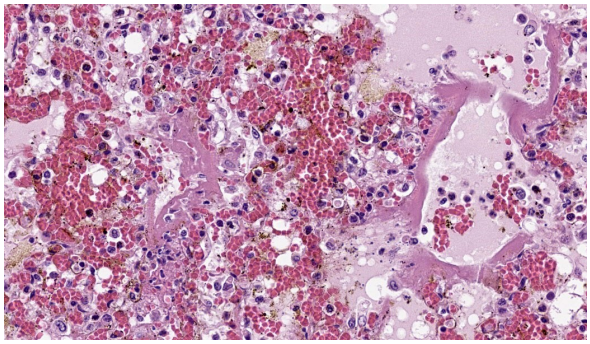

Figure 1-6. Lung, donkey: Compacted fibrin lines alveolar septa (hyaline membranes). (HE, 773X)

JPC Comment:

The 20th conference of the 2025-2026 Wednesday Slide Conference was moderated by the wonderful Dr. Patty Pesavento, from the University of California, Davis. This first case was a fantastic example of equine influenza with a secondary bacterial infection, and the contributor provided a fantastic writeup for this entity.

Determining differentials in a case of viral pneumonia in any species requires a working knowledge of viral pathogenesis and target cells to refine the list of potential offenders. In this case, the most striking hallmarks for influenza virus include the end-airway epithelial necrosis and patchy areas of hemorrhage. Influenza is both endotheliotropic and epitheliotropic and, while it affects epithelial cells in the upper airways, it has unique tropism for the type I and type II pneumocytes of the alveoli as well. It causes significant destruction to end-airways as a result. This key difference can help separate an influenza infection from other pneumotropic viruses, such as calicivirus in cats. (Feline calicivirus infection of the lung can look nearly identical to an H5N1 influenza virus infection in a cat, but the state of the end airways can help clue in the pathologist to which virus is most likely and can assist in decision-making for next testing steps. The more virulent strains of feline calicivirus can cause severe interstitial pneumonia, but they do not cause necrosis of end airways the way that influenza does.)

Grossly, an influenza-infected lung has a "checkerboard" appearance with random, alternating areas of dark red atelectasis and light pink, aerated lung. This pattern manifests because influenza does not uniformly infect every cell it comes into contact with due to varied densities of sialic acid receptors on the host cells. Dark red to purple areas of consolidation represent collapsed alveoli whose airway has been clogged by exudate and which can no longer pass air through to the alveoli.. These solidified, dark red sections contrast sharply with the lighter-colored, air-filled alveoli.

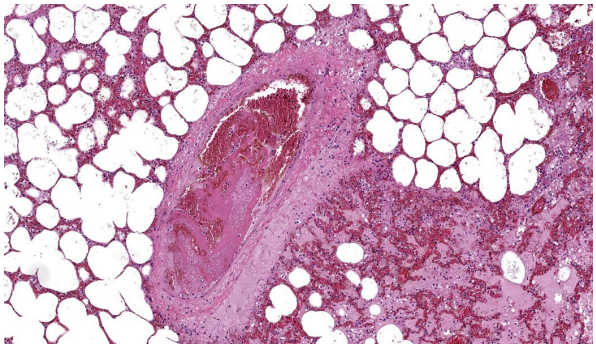

Figure 1-7. Lung, donkey: A pulmonary vein contains a large occlusive fibrin thrombus (HE, 162X)

As stated by the contributor, donkeys are more susceptible to equine influenza virus than horses, although both species primarily develop respiratory disease with influenza.[1] This is true in pigs and humans, as well, where the lung is the main target of influenza.

In cats, however, the primary presentation of influenza, especially H5N1, is encephalitis. Cats are also susceptible to cerebral infarcts from influenza targeting vascular endothelium. Swine can also be infected with neurotropic strains of influenza A, including H5N1. One of the main mechanisms for infection with H5N1 influenza in cats is consumption of contaminated cow's milk.[9]

In cattle, the primary targets for influenza are the mammary glands due to high tropism for and concentration of the virus in bovine mammary gland epithelium with subsequent shedding of the virus into milk.[9] It is unclear if this is true in other species, but it has been definitively demonstrated that, in humans, the virus does not target the mammary glands.[9] Additionally, modern pasteurization

and homogenization methods used in most commercial dairies completely kills any influenza virus that may be present in cow milk, so milk from dairies that use these methods is still very much safe for human consumption.[9] In birds, the primary cellular targets for influenza, especially highly pathogenic avian influenza, are the brain and pancreas. Avian influenza was discussed more in depth in this year's Conference #17, Case 2.

All participants considered the bacterial infection to be secondary and due to aerogenous introduction of bacteria into an already virus-infected lung. This ruled out *Streptococcus spp,* including *S. equi* or *S. zooepidemicus,* as contributing to the bacterial infection, as these spread hematogenously.

References:

1. Ahearne MM, Pentzke-Lemus LL, Romano AM, Larsen ED, Watson AM, O'Fallon EA, Landolt GA. Disease progression, pathologic, and virologic findings of an equine influenza outbreak in rescue donkeys. *J Vet Intern Med*. 2022; 36(6):2230-2237.

2. Boyle AG, Timoney JF, Newton JR, Hines MT, Waller AS, Buchanan BR. Streptococcus equi Infections in Horses: Guidelines for Treatment, Control, and Prevention of Strangles-Revised Consensus Statement. *J Vet Intern Med*. 2018;32 (2):633-647.

3. Câmara RJF, Bueno BL, Resende CF, Balasuriya UBR, Sakamoto SM, Reis JKPD. Viral Diseases that Affect Donkeys and Mules. *Animals* (Basel). 2020;25;10(12):2203.

4. Carvallo FR, Stevenson VB. Interstitial pneumonia and diffuse alveolar damage in domestic animals. *Vet Pathol*. 2022;59 (4):586-601.

5. Carvallo FR, Uzal FA, Diab SS, Hill AE, Arthur RM. Retrospective study of fatal pneumonia in racehorses. *J Vet Diagn Invest*. 2017;29(4):450-456.

6. Chambers TM. Equine Influenza. *Cold Spring Harb Perspect Med*. 2022; 4;12 (1):a038331.

7. Crawford PC, Dubovi EJ, Castleman WL, Stephenson I, Gibbs EP, Chen L, Smith C, Hill RC, Ferro P, Pompey J, Bright RA, Medina MJ, Johnson CM, Olsen CW, Cox NJ, Klimov AI, Katz JM, Donis RO. Transmission of equine influenza virus to dogs. *Science*. 2005; 21;310(5747):482-5.

8. Dionísio L, Medeiros F, Pequito M, Faustino-Rocha AI. Equine influenza: a comprehensive review from etiology to treatment. *Anim Health Res Rev*. 2021; 22(1):56-71.

9. Landolt GA. Equine influenza virus. *Vet Clin North Am Equine Pract*. 2014; 30 (3):507-22.

10. Rahman A, Uzal FA, Hassebroek AM, Carvallo FR. Retrospective study of pneumonia in non-racing horses in California. *J Vet Diagn Invest*. 2022; 34 (4):587-593.

11. Singh RK, Dhama K, Karthik K, Khandia R, Munjal A, Khurana SK, Chakraborty S, Malik YS, Virmani N, Singh R, Tripathi BN, Munir M, van der Kolk JH. A Comprehensive Review on Equine Influenza Virus: Etiology, Epidemiology, Pathobiology, Advances in Developing Diagnostics, Vaccines, and Control Strategies. *Front Microbiol*. 2018; 6(9):1941.

12. Timoney PJ. Equine influenza. *Comp Immunol Microbiol Infect Dis*. 1996; 19 (3):205-11.

13. Yang H, Xiao Y, Meng F, Sun F, Chen M, Cheng Z, Chen Y, Liu S, Chen H. Emergence of H3N8 equine influenza virus in donkeys in China in 2017. *Vet Microbiol.* 2018; 214:1-6.

14. Xie T, Anderson BD, Daramragchaa U, Chuluunbaatar M, Gray GC. A Review of Evidence that Equine Influenza Viruses Are Zoonotic. *Pathogens*. 2016; 12;5 (3):50.

CASE II:

Signalment:

4-year-old, male, Balinese cat, (*Felis silvestris catus)*

History:

Sudden death**,** after one month in which the subject manifested increased appetite.

Gross Pathology:

At necropsy, multiple organs were affected:

Abdominal cavity: in the cavity there was an effusion (approx. 30 ml) of pale, yellow, and transparent fluid which contained scattered strands of white, elastic, and insoluble material (fibrin).

On the serosal surfaces of the major abdominal and thoracic organs (spleen, kidneys, intestine, pancreas, lungs and heart) there were multifocal, well defined, irregularly round, raised, white, and compact plaques that varied in size from few millimeters to a centimeter in major diameter. Some of these lesions extended into the parenchyma of organs and presented poorly defined and irregular edges.

Thoracic cavity: the same fluid (approx. 10 ml) was found in the thoracic cavity.

Trachea: There was moderate intraluminal white-pink foam (edema). Lungs: multifocal, white, solid, slightly protruding lesions up to few millimeters in diameter were present under the pleura. At cut surface, they showed irregular well-defined margins and white coloration.

Liver: The serosal surface of the organ was covered by extensive and abundant yellow, firm material, with a granular superficial appearance. On cut surface, the material did not extend into the parenchyma. Many multifocal friable yellow adhesions were present between the liver and the wall of the abdominal cavity.

Lymph nodes: Thoracic and abdominal lymph nodes were enlarged, dark red, and firm. At cut surface, they presented a diffuse homogenous dark red coloration. The macroscopic morphological diagnosis was therefore: diffuse and severe fibrinous peritonitis and pleuritis with generalized severe hemorrhagic lymphadenitis.

Laboratory Results: N/A

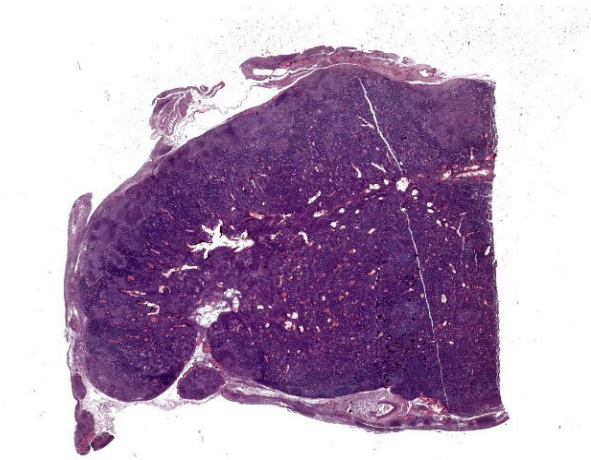

2-1. Lymph node, cat. A partial section of a markedly enlarge lymph node is submitted for examination. There is loss of the normal nodal architecture. (HE, 9X)

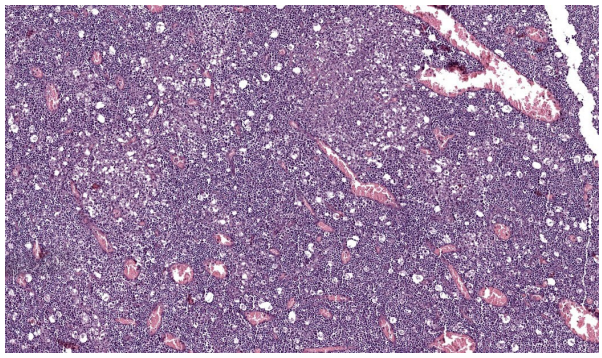

2-2. Lymph node, cat. There is marked expansion of the paracortex with loss of germinal centers. Numerous tingible body macrophages and apoptotic lymphocytes give the node a "starry sky"

Microscopic Description:

Abdominal lymph node: Multifocal, severe cellular infiltrates with undefined margins are randomly distributed within the lymph node parenchyma especially in the subcapsular areas. They extend into the serosal expanding and effacing the mesothelial lining. The infiltrates are characterized by a severe mixed inflammatory population with large-numbers of both viable and lytic neutrophils surrounded by occasional large macrophages with abundant cytoplasm and rare lymphocytes and plasma cells. In the center of almost each infiltrate the neutrophils population shows karyolysis, pyknosis, karyorrhexis and the accumulation of extensive amount of amorphous eosinophilic, proteinaceous material admixed with cellular debris (lytic necrosis).

Immunohistochemical (IHC) staining of lymph node sections using a mouse anti-Feline Coronavirus antibody (clone FIPV3-70 Serotec, Oxford UK) demonstrates strong positivity for many elements within the inflammatory infiltrates, suggestive of presence of viral antigen.

Contributor's Morphologic Diagnosis: Multifocal severe necrotizing and piogranulomatous lymphadenitis and peritonitis associated with Feline Coronavirus antigen. Feline infectious peritonitis.

Additional findings:

- Diffuse severe peritonitis
- Multifocal severe piogranulomatous hepatitis, pneumonia, pancreatitis, nephritis,myocarditis and enteritis.
- Lung: Mild diffuse edema and mild diffuse emphysema
- Liver: Diffuse, severe hepatic hydropic degeneration.

Contributor's Comment:

Feline infectious peritonitis (FIP) is an uncommon, fatal, progressive, and immune-mediated disease of cats caused by feline coronavirus (FCoV) infection. At present, despite decades of research on its etiology, pathogenesis, transmission, and prevention, FIP is still one of the most frequent fatal and infectious feline disease for which there is, so far, no effective cure.[1]

Infection with FCoV is common in cats throughout the world, although, in most cats, the virus causes no clinical signs. However, in some cats, FCoV infection is associated with the development of the progressive and fatal disease manifestation of FIP.[3]

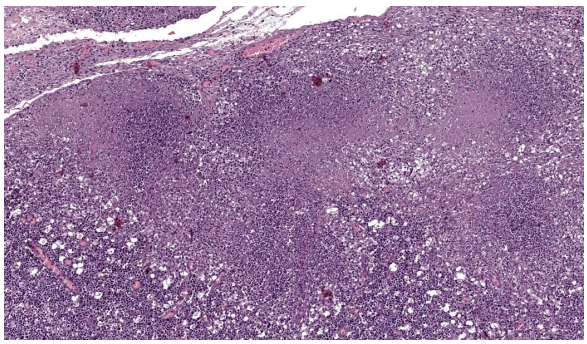

Figure 2-3. Lymph node, cat. Lymph node, cat There are numerous coalescing areas of lytic necrosis within the expanded paracortex. (HE, 114X)

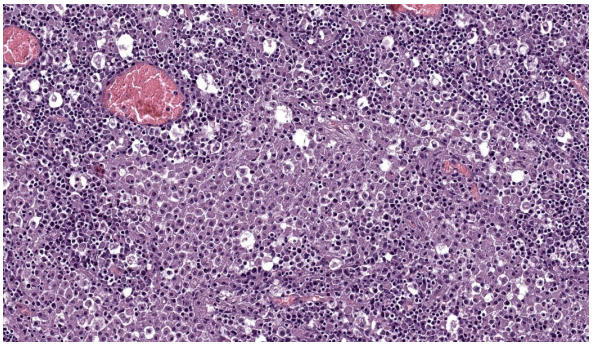

Figure 2-4. Lymph node, cat. There are extensive areas of granulomatous inflammation scattered throughout the cortex. (HE, 381X)

The current knowledge of genetic differences between feline enteric coronaviruses (FECV) and feline infectious peritonitis virus (FIPV) has been mainly based on comparative sequence analyses that revealed "discriminatory" mutations that are present in FIPVs but not in FECVs.[6] Most of these mutations result in amino acid substitutions in the S protein and these may have a critical role in the switch from FECV to FIPV.[1] In most cases, the precise roles of these mutations in the molecular pathogenesis of FIP have not been tested experimentally in the natural host, mainly due to the lack of suitable experimental tools including genetically engineered virus mutants.[6]

Cats that do not clear FIPV develop either dry or wet forms of the disease depending on whether ineffective cell-mediated or humoral immunity dominates the clinical disease. Although often described as distinct entities, the effusive and non-effusive forms of FIP are the farthest of a continuum of syndromes, characterized by vasculitis and pyogranulomatous inflammation. Effusive disease is more common than the non-effusive form, and mixed forms are common.[6] In our case clear indication of vasculitis was not present and necrosis was diffusely associated with the pyogranulomatous infiltrate, therefore IHC was needed to confirm the etiology.

Contributing Institution:

Dept. Comparative Biomedicine and Food Science (BCA) -
Veterinary Medicine - University of Padua
AGRIPOLIS - Viale dell'Università 16
35020 Legnaro (PD) - Italy
http://www.bca.unipd.it/en/

JPC Morphologic Diagnosis:

Lymph node: Lymphadenitis and capsulitis, necrotizing and granulomatous, chronic, multifocal to coalescing, marked, with paracortical hyperplasia.

JPC Comment:

This case was an excellent representation of a real-life manifestation of FIP, as classic vasculitis was not a significant part of this lesion (although areas of necrosis within the node suggested the presence of vascular damage. The top differentials for participants included FIP, *Francisella tularensis*, and *Yersinia pestis* (causative agent of bubonic plague) and other "hot" gram-negatives, and less commonly, and rare cases of feline parvovirus infection. The Pesavento Laboratory confirmed the positive

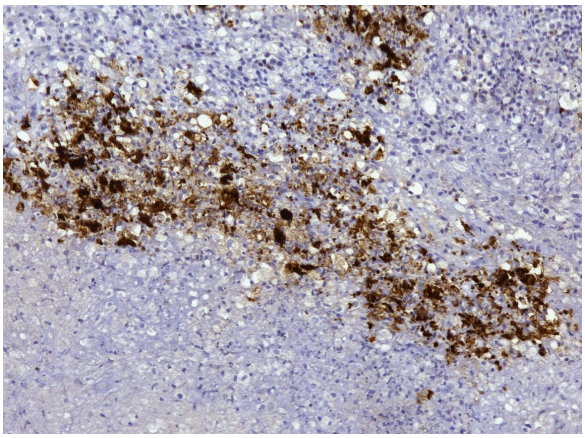

Figure 2.5. Lymph node, cat. Areas of granulomatous inflammation demonstrate strong immunostaining against coronaviral antigen (anti-FIPV3-70, 200X) (*Photo courtesy of*: Dept. Comparative Biomedicine and Food Science (BCA), Veterinary Medicine - University of Padua, http://www.bca.unipd.it/en/).

immunohistochemical identification of coronavirus in this case using a canine coronavirus antibody which cross reacts with many other related coronaviruses.

FIP is globally distributed and fatal if untreated. Today, however, antiviral treatment is over 80% effective.[4] Certain breeds are more susceptible to infection, but the gene association in the host has not yet been identified.[8] FIPV can cause disease in exotic big cat species as well, and has been reported in lions, servals, cheetahs, mountain lions, and others.[2,5,7,9,10]

Dr. Pesavento discussed how much we still have to learn about FIP, including the triggers of viral activation, how FIP persists in a host, the host range, susceptibility factors, and how variable manifestations of infection affect the outcome for the individual. While 98% of cats infected with FeCoV never develop FIP, what exactly causes or triggers the genetic mutations that result in FIP is still unknown. The general cause of FIP is enteric persistence of FeCoV within a host, specifically within the colon, coupled with systemic access and mutation of the virus into a pathogenic FIPV. There are multiple mutations and multiple genes involved in this transformation of FeCoV into FIPV, many of which are not fully understood.

Additionally, a phenomenon known as "antibody-dependent enhancement" has been demonstrated in cats that are re-infected with an identical serotype of FIPV.[11] Antibody-dependent enhancement (ADE) is a phenomenon in which non-neutralizing or weak antibodies bind to a virus but fail to neutralize it. Instead, the antibody actually facilitates the virus' entry into cells, resulting in increased viral replication and more severe disease.[11] This makes this disease particularly challenging for vaccine development. Currently vaccine development targets the nucleocapsid (N) protein. This N protein is well-conserved across coronaviral strains, unlike the spike (S) protein that is prone to significant variation. The N protein can trigger a longer-lasting antibody response, but, perhaps more importantly, an N-specific cytotoxic T lymphocyte response. This elegant targeting of a cell-mediated, rather than a humoral, response may help avoid antibody-dependent enhancement in FIPV.

References:

1. Brown MA, Troyer JL, Pecon-Slattery J, Roelke ME, O'Brien SJ. Genetics and Pathogenesis of Feline Infectious Peritonitis Virus. *Emerg Infec Dis*. 2009;15 (9):1445-1452

2. Evermann JF, Heeney JL, Roelke ME, McKeirnan AJ, O'Brien SJ. Biological and pathological consequences of feline infectious peritonitis virus infection in the cheetah. *Arch Virol*. 1988;102(3-4):155-171.

3. Giordano A, Paltrinieri S, Bertazzolo W, Milesi E, Parodi M. Sensitivity of Trucut and fine-needle aspiration biopsies of liver and kidney for diagnosis of feline infectious peritonitis. *Vet Clin Path*. 2005;34(4):368-374.

4. Kipar A, Meli ML. Feline Infectious Peritonitis: Still an Enigma? *Vet Path*. 2014;51 (2):505-526.

5. Juan-Sallés C, Domingo M, Herráez P, Fernández A, Segalés J, Fernández J. Feline infectious peritonitis in servals (Felis serval). *Vet Rec*. 1998;143(19):535 -536.

6. Kipar A, Meli ML. Feline Infectious Peritonitis: Still an Enigma? *Vet Path*. 2014;51 (2):505-526.

7. Mwase M, Shimada K, Mumba C, Yabe

J, Squarre D, Madarame H. Positive immunolabelling for feline infectious peritonitis in an African lion (Panthera leo) with bilateral panuveitis. *J Comp Pathol*. 2015;152(2-3):265-268.

8. Pesteanu-Somogyi LD, Radzai C, Pressler BM. Prevalence of feline infectious peritonitis in specific cat breeds. *J Feline Med Surg*. 2006;8(1):1-5.

9. Stephenson N, Swift P, Moeller RB, Worth SJ, Foley J. Feline infectious peritonitis in a mountain lion (Puma concolor), California, USA. *J Wildl Dis*. 2013;49(2):408-412.

10. Stout AE, André NM, Whittaker GR. Feline coronavirus and feline infectious peritonitis in nondomestic felid species. *J Zoo Wildl Med*. 2021;52(1):14-27.

11. Takano T, Kawakami C, Yamada S, Satoh R, Hohdatsu T. Antibody-dependent enhancement occurs upon re-infection with the identical serotype virus in feline infectious peritonitis virus infection. *J Vet Med Sci*. 2008;70 (12):1315-1321.

CASE III:

Signalment:

5-month-old, female black-winged starling (*Acridotheres melanopterus*)

History:

This was a parent-raised bird hatched in a mixed species aviary. It was found dead in the habitat with no previous clinical history.

Gross Pathology:

Postmortem and body condition were good with mild autolysis and moderate fat stores. The liver was enlarged filling much of the coelomic cavity and mottled shades of tan and brown. The spleen was enlarged at 3 x 0.5 x 0.5 cm. The upper gastrointestinal tract was empty and the small and large intestinal loops were diffusely mildly dilated.

Laboratory Results:

In-house cPCR assays with sequencing (frozen lung and duodenum):

- Isospora-specific cytochrome *c* oxidase: *Isospora serini* (BLAST Accession ON584773), 96.7-96.9% identical
- Trichomonas 18S rRNA: *Cochlosoma anatis* (BLAST Accession AY247745), 92.7% identical

Electron microscopy, California Animal Health and Food Safety Lab in Davis, CA (formalin-fixed liver):

- Free organisms- family *Trichomonadidae* flagellates with 5 apical flagella (one recurrent)
- Lymphocytes- Intracytoplasmic *Isospora*

Microscopic Description:

Liver: Surrounding portal regions and occasionally coalescing are infiltrates of moderate numbers of lymphocytes and histiocytes that disrupt the hepatic architecture. Within the lymphocytes and histiocytes are numerous, 2um in diameter, basophilic protozoal organisms surrounded by a thin, clear halo that peripheralizes the nucleus. The inflammatory cells separate and individualize the hepatocytes, which display mild karyomegaly and frequent binucleation. Free within the sinusoidal lumina and within portal and central veins are numerous, approximately 5 um diameter, pyriform flagellate protozoa with a single, variably distinct nucleus. Occasional large lymphocytes and rare plasma cells circulate throughout the sinusoids.

Duodenum: The mucosal lamina propria is

markedly infiltrated and expanded by numerous lymphocytes and histiocytes with rare plasma cells. The inflammatory cells broaden and occasionally fuse the villi and separate the intestinal crypts. Within the mononuclear cells are abundant 2um diameter, basophilic protozoal organisms surrounded by a thin, clear halo that peripheralizes and indents the nucleus. The crypt epithelial cells are often pyknotic and sloughed into the lumen. Epithelial cells at the crypt bases are often hyperplastic, piling three to four cells thick with increased numbers of mitotic figures. The coelomic fat surrounding the duodenum has small, multifocal aggregates of lymphocytes.

Cloaca, colon, and bursa of Fabricius: The lamina propria of the colon is infiltrated and expanded by moderate numbers of lymphocytes and plasma cells that separate colonic crypts. Multifocal crypts are filled with numerous, approximately 5 um diameter, pyriform flagellates with a single, variably distinct nucleus. Similar flagellates are also identified in large numbers within the lumen. Within the bursa of Fabricius, there are similar trichomonad flagellates as well as approximately 2-3 um diameter, round, protozoal organisms that are often adhered to the superficial surface of the epithelial cells.

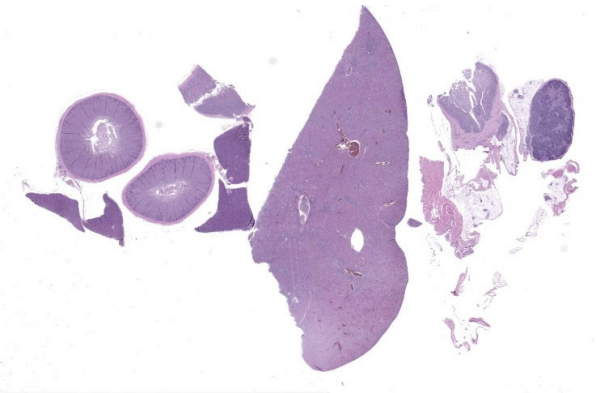

3-1. Abdominal viscera, starling: Sections from the gastrointestinal tract to include liver, duodenum, pancreas, cloaca and bursa are submitted for examination.

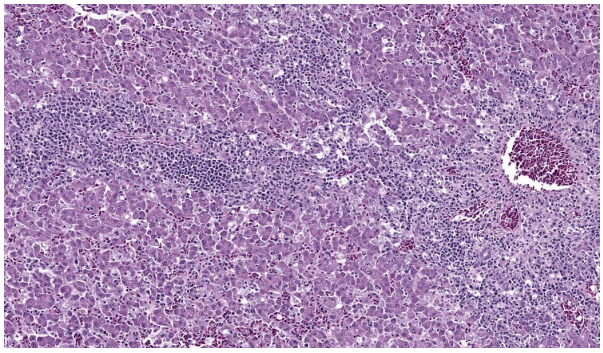

Figure 3-2. Liver, starling: There is marked inflammation centered on portal areas, which is composed of large numbers of macrophages, lymphocytes and plasma cells which crosses the limiting plate and extends into the adjacent hepatic parenchyma. (HE, 279X).

Contributor's Morphologic Diagnosis:

Liver: Moderate, multifocal, chronic, lymphohistiocytic hepatitis with intracellular protozoa (consistent with isosporosis, *Isospora* sp) and sinusoidal flagellates
Duodenum: severe, chronic, segmental, histiocytic enteritis, with abundant intracellular protozoa (consistent with isosporosis, *Isospora* sp.)
Cloaca and bursa of Fabricius: moderate, chronic, proliferative and lymphoplasmacytic cloacitis and bursitis with superficial mucosal protozoa, consistent with cryptosporidiosis, *Cryptosporidium* sp.
Colon and cloaca: myriad crypt and luminal flagellates

Contributor's Comment:

This young black-winged starling had two clinically significant systemic protozoal infections, confirmed by PCR assays and electron microscopy, that likely led to its death. A third suspected protozoal infection was seen histologically in the cloaca and bursa of Fabricius but not confirmed with ancillary testing. Gizzard candidiasis completed the picture of a bird with an immature or deficient immune system despite its apparently

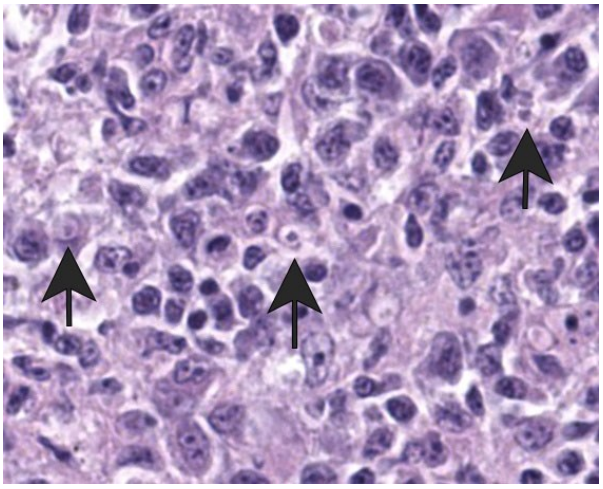

3-3. Liver, starling: Macrophages and lymphocytes occasionally contain a single cytoplasmic protozoal zoite consistent with *Sarcocystis spp.* which measures 2-3um and often peripheralizes or compresses the nucleus. (HE, 1793X).

adequate nutritional status.

Systemic isosporosis was identified histologically and cytologically in histiocytes and lymphocytes of an inflammatory response affecting small intestine, liver, spleen, and other tissues. Isosporosis is well-described in captive and free-range passerines. Formerly known as atoxoplasmosis, the pathogenesis of systemic isosporosis remains uncertain but involves extraintestinal invasion of mononuclear cells by sporozoites that undergo asexual reproduction. It is endemic in populations of passerines with fatal infections associated with stress, concurrent infections, or immunosuppression.[3] Mortality due to *Isospora sp* in wild birds is low, however, mortality in captive birds is significantly higher. Stress due to captivity and increased shedding of infective oocysts have been proposed as possible causes for the higher mortality observed in captive passerines.[3] As seen in this case, isosporosis is most commonly seen in the proximal segments of the small intestine and is accompanied by infiltration by mononuclear cells. Compromise to the intestinal mucosa as a result of the severe inflammation in this case could have led to invasion by the second protozoal infection.

Present in often very large numbers throughout the vasculature were extracellular protozoa consistent with flagellates that could have contributed to the inflammation in some tissues. Using a trichomonad PCR assay, sequences with a closest match to *Cochlosoma anatis* were obtained from both lung and intestine, although identity was only ~93%. Electron microscopy of liver tissue confirmed intracellular protozoa consistent with *Isospora*, and extracellular flagellates consistent with tetratrichomonads based on the presence of 5 undulipodia at the apical pole with one recurrent. In contrast, *Cochlosoma* sp. have six flagella, one of which is recurrent. Both *Cochlosoma* and *Trichomonas* have a single nucleus, a parabasal apparatus, a tubular axostyle, and a crescent-shaped pelta.[6] Prior studies have identified via sequence analysis of the 16S rRNA gene that *Cochlosoma* and *Trichomonas* are genetically similar, which likely accounts for the 93% identity match.[4] *Tetratrichomonas* and *C. anatis* are often identified with other intestinal pathogens and their pathogenicity as a sole pathogen remains uncertain.[1,4] Both have been documented as the cause of fulmi-

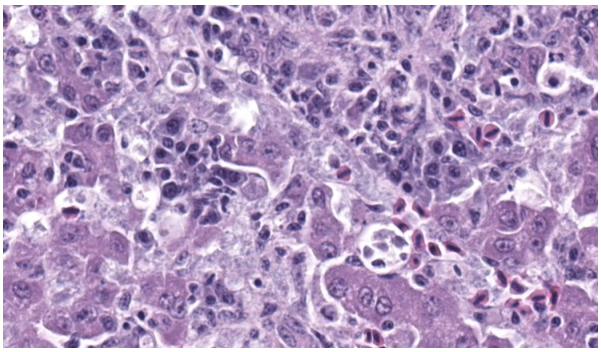

Figure 3-4. Liver, starling: Within portal areas, macrophages also contain multiple 2-4um pyriform flagellates within their cytoplasm. (HE, 1493X)

nant disease in a variety of birds. Tetratrichomoniasis has been identified as the causative agent of acute typhlohepatitis in ducks, a necrotizing hepatitis and splenitis in a Waldrapp ibis and necrotizing hepatitis in a free-ranging white pelican.[1,2] *Cochlosoma anatis* is linked to enteritis in turkeys, as well as increased dehydration, malabsorption, and mortality in young finches.[4] However, prior studies have failed to document clinical signs or histologic lesions in experimental infections with *Trichomonas* and coinfections of *Cochlosoma* with other intestinal pathogens have demonstrated greater pathogenicity than with either pathogen alone.[1,4]

Flagellates were also present in the colonic and cloacal lumen, including deep in the crypts. In this location, their visualization was complicated by suspected cryptosporidiosis, the third protozoal infection, which was best seen in the bursa of Fabricius. The cryptosporidiosis within the bursa of Fabricius was not confirmed via ancillary diagnostics, but the appearance in this location was typical, though less common than proventricular cryptosporidiosis in passerines. The colonization of the bursa by the *Cryptosporidium*

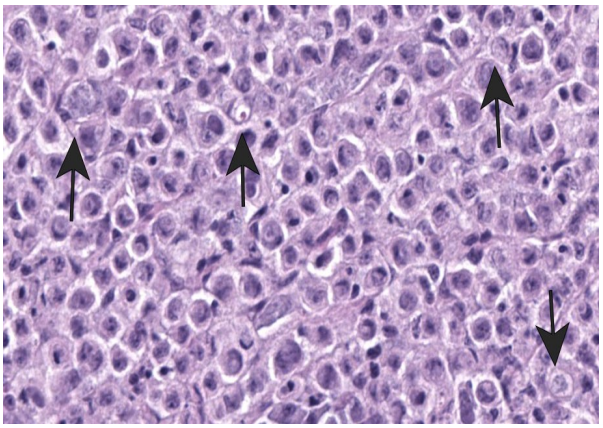

Figure 3-5. Duodenum, starling: The lamina propria is expanded by large numbers of macrophages which surround, separate, and often efface crypts. (HE, 279X)

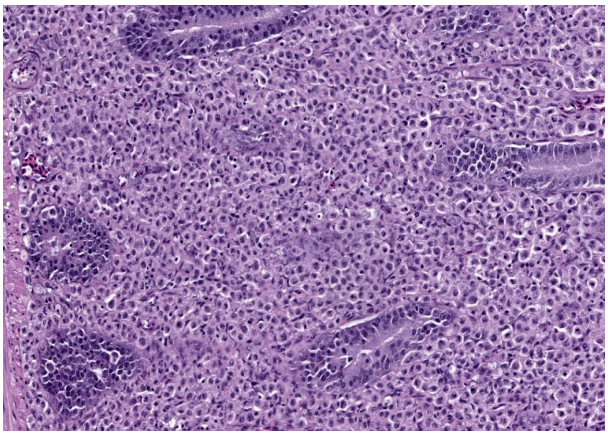

Figure 3-6. Duodenum, starling; Macrophages occasionally contain a single cytoplasmic protozoal zoite consistent with *Sarcocystis spp.* which measures 2-3um and often peripheralizes or compresses the nucleus. (HE, 1793X).

and the resulting bursitis may have impaired the humoral immune response, further predisposing the starling to the multiple concurrent protozoal infections.

Contributing Institution:

Disease Investigations
San Diego Zoo Wildlife Alliance
PO Box 120551
San Diego, CA 92112
https://science.sandiegozoo.org/disease-investigations

JPC Morphologic Diagnosis:

1. Liver: Cholangiohepatitis, histiocytic and lymphoplasmacytic, chronic, diffuse, marked, with intrahistiocytic apicomplexan zoites and sinusoidal flagellates.
2. Duodenum: Enteritis, histiocytic, chronic, diffuse, severe, with intrahistiocytic apicomplexan zoites.
3. Cloaca: Cloacitis, proliferative and histiocytic, chronic, diffuse, marked, with numerous luminal flagellates.
4. Bursa of Fabricius: Bursitis, necrotizing, chronic, multifocal, mild, with intraluminal flagellates.

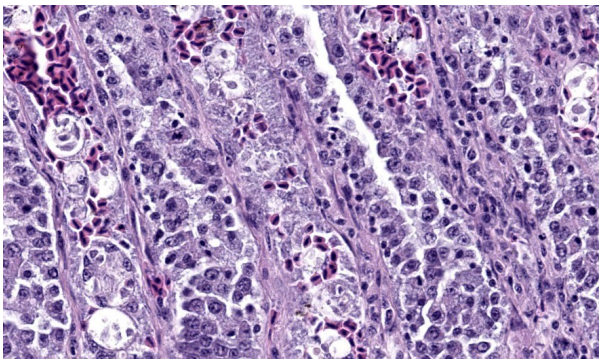

Figure 3-7. Cloaca: There are numerous 2-4um pyriform protozoa within the glands and occasionally with macrophages cytoplasm. (HE 864X)

JPC Comment:

Many thanks to this contributor for an interesting case and well-written comment! It has been a while since the WSC saw a case of atoxoplasmosis (WSC 2009, Conf 18, Case 3), and this case provided some excellent discussion points. This was a challenging slide for many participants due to the lymphoproliferative nature of this protozoal infection, which, depending on the severity of the infection and the species affected, can be confused with lymphoma caused by gallid herpesvirus-2 (Marek's disease), and avian retrovirus (lymphoid leukosis), etc.[3] This was true in this conference, and some participants wondered about a lymphoma as the primary disease with the protozoa being secondary. The *Isospora serini* were easier for the participants to find in this collection of tissue, but finding the flagellates, (*Cochlosoma anatis*) proved more difficult on the HE section (however, once the first flagellate were identified, participants were able to find them with ease.) Flagellates have a small, pinpoint nucleus and piriform shape, which differentiates them from mucin and debris. The group decided that there was not definitive evidence of cryptosporidia on the section of bursa, but only a very limited area of bursal epithelium (which cryptosporidia invade) was present in the section, so sampling was extremely limited.

This case provided a nice example of granulopoiesis in the liver, characterized by granulocytes that lacked a bilobed nucleus and clustered with hematopoietic precursors. It is easy to overlook or over-interpret extramedullary hematopoiesis, but knowing which species it is normally and commonly seen in is important. Birds, reptiles, and some rodents can routinely have foci of EMH in their livers. There was additionally some beautiful tertiary lymphoid follicle development in this case secondary to the chronic inflammation!

Evaluation of the bursa of Fabricius proved to be an important point of discussion. The bursa naturally involutes as birds age and should be a synchronous process.[7] In chickens, the Bursa begins involution around 8-10 weeks of age and is generally heavily involuted by 6-7mo old.[7] In this case, however, there was asynchronous depletion of the Bursa, indicating that this was not natural involution. There were some follicles that exhibited lytic central necrosis and lymphocytolysis, demonstrating an active insult to the Bursa that may have contributed to this

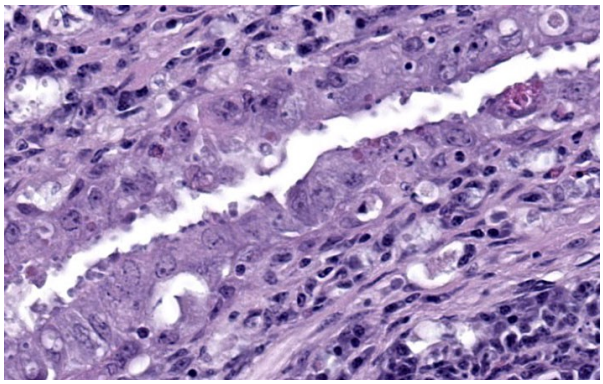

Figure 3-8. Bursa of Fabricius, starling: There are numerous cryptosporidial meronts and gamonts within the apical cytoplasm (intracellular, extracytoplasmic) of epithelial cells. (HE, 1072X)

bird's immunosuppression. Whether this was viral or parasitic could not be determined. Although participants were not convinced about *Cryptosporidium spp.*, the bursal epithelium are good places to hunt for them since the bursa of Fabricius is a continuation of the intestine. In trying to put a pathogenesis together in this case, participants thought that the most likely primary cause of this bird's demise was nutritional malabsorption due to the marked histiocytic enteritis with epithelial necrosis and crypt separation.

Finally, Dr. Pesavento quizzed participants on the ultrastructural images from this case, which was an appreciated, succinct review for many attendees. Key takeaways from this discussion included trusting your anchors (i.e. erythrocytes, nuclei, etc.), determining the number of cell profiles in the EM image, and knowing what normal looks like so you can evaluate the abnormal. The protozoal organisms on EM had some key characteristics to look for, as well, including the flagella on the trichomonads with their classic microtubule 9+2 arrangement, and the apicomplexan conoid, rhoptries, and micronemes within the *Isospora*.[5,6] Her last piece of wisdom in this case regarded microvilli on EM: don't call them microvilli unless you can see the actin microfilaments holding them up. If not, they are termed "cellular projections."

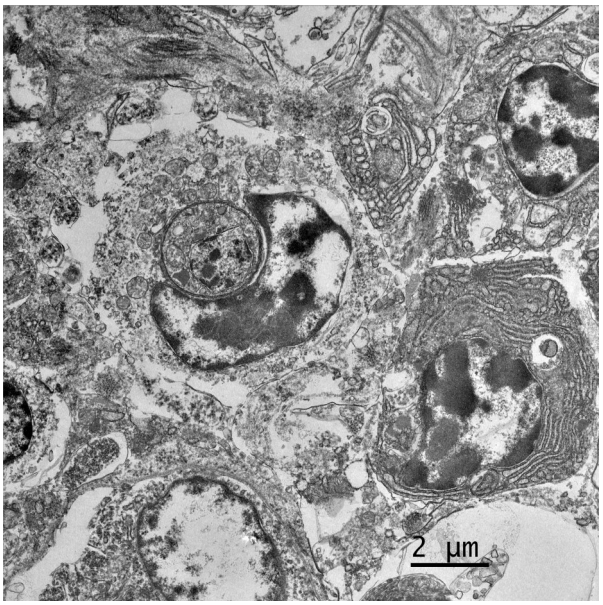

Figure 3-9. Liver, starling: An ultrastructural photomicrograph demonstrates a single apicomplexan schizont with the cytoplasm of a macrophage. A plasma cell is at right. (Photo courtesy of Disease Investigations, San Diego Zoo Wildlife Alliance, https://science.sandiegozoo.org/disease-investigations)

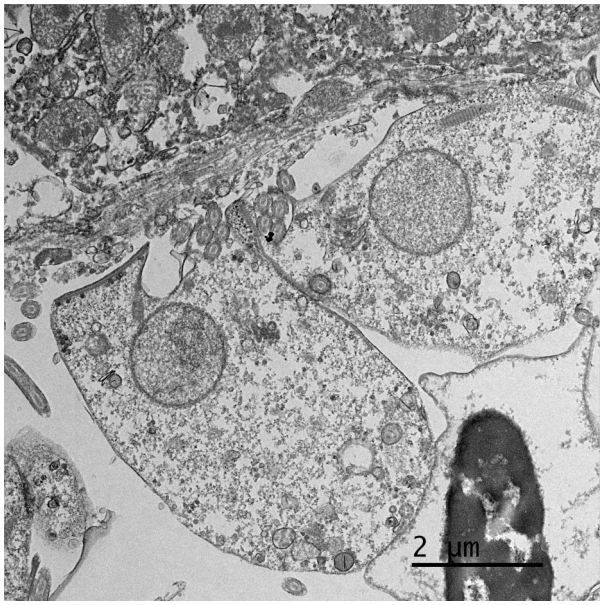

Figure 3-10. Cloaca, starling: An ultrastructural photomicrograph demonstrates two flagellates within the lumen of the cloaca. Numerous cross sections of flagella may be seen at th periphery of the flagellates. (Photo courtesy of Disease Investigations, San Diego Zoo Wildlife Alliance, https://science.sandiegozoo.org/disease-investigations)

References:

1. Amin A, Bilic I, Liebhardt D, Hess M. Trichomonads in birds – a review. *Parasitol*. 2014;141(6):733-747.

2. Burns RE, Braun J, Armien AG, Rideout BA. Hepatitis and splenitis due to systemic tetratrichomoniasis in an American white pelican (*Pelecanus erythrorhynchos*). *J Vet Diagn Invest*. 2013;2(4):511-4.

3. Cushing TL, Schat KA, States SL, Grodio JL, O'Connell PH, Buckles EL.

Characterization of the host response in systemic Isosporosis (Atoxoplasmosis) in a colony of captive American goldfinches (*Spinus tristis*) and house sparrows (*Passer domesticus*). *Vet Pathol.* 2011;48(5):985-992.

4. Evans NP, Evans RD, Fitz-Coy S, Pierson FW, Robertson JL, Lindsay DS. Identification of new morphological and life-cycle stages of *Cochlosoma anatis* and experimental transmission using pseudocyst. *Avian Dis*. 2006;50(1):22-27.

5. Udoumoh AF, Nwaogu IC, Igwebuike UM, Obidike IR. Pre-hatch and post-hatch development of the bursa of Fabricius in broiler chicken: a morphological study. Vet Res Forum. 2022 Sep;13 (3):301-308.

6. Pecka Z, Nohýnková E, Kulda J. Ultrastructure of *Cochlosoma anatis* (Kotlán, 1923) and taxonomic position of the family Cochlosomatidae (parabasala: Trichomonadida). *Eur J Protistol*. 1996;32(2):190-201.

7. Udoumoh AF, Nwaogu IC, Igwebuike UM, Obidike IR. Pre-hatch and post-hatch development of the bursa of Fabricius in broiler chicken: a morphological study. Vet Res Forum. 2022 Sep;13 (3):301-308.

CASE IV:

Signalment:

5-year-old, female-spayed , mixed-breed dog (*Canis familiaris*)

History:

The patient presented to a veterinary medical teaching hospital with left-sided hemiparesis, acute onset of bilateral blindness and circling to the right. Bloodwork revealed no significant abnormalities. Upon hospital admission, the patient's obtundation progressed to stupor so euthanasia was elected . The owners reported that the patient had no significant clinical history other than diagnosis of and recovery from canine distemper at 1-year-old.

Gross Pathology:

No significant gross abnormalities were appreciated.

Laboratory Results:

Canine distemper virus (Brain): Neurons and, less frequently, astrocytes exhibit strong cytoplasmic immunoreactivity.

Special stains: Luxol fast blue (Brain): Decreased positive staining supports demyelination of the cortical white matter.

Microscopic Description:

The slide contains one section of cerebrum at the level of the basal nuclei and corpus callosum. The white matter and, to a lesser extent, grey matter are moderately vacuolated and hypercellular. Vacuolation is defined by clear, well-demarcated vacuoles that reach up to 50 um diameter

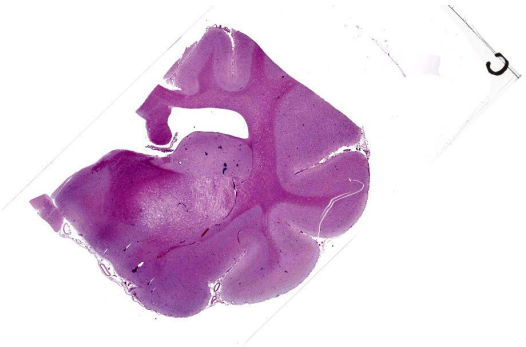

Figure 4-1. Cerebrum, dog: A section of cerebrum through the corpus callosum and thalmusis submitted for examination. At subgross magnification perivascular cuffing of thalamic vessels is visible. (HE, 8X)

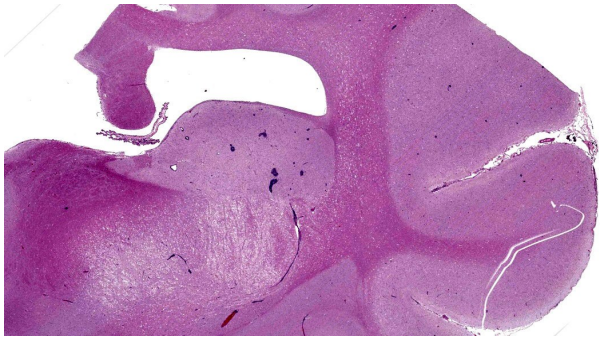

Figure 4-2. Cerebrum, dog: At low magnification, marked spongiosis of the thalamic white matter and to a lesser extent, the internal capsule is visible. (HE, 12X)

(spongiosis). The neuropil is additionally disrupted by increased numbers of proliferating glial cells (gliosis). Parenchymal vacuolation and gliosis of the grey matter is less severe than that described within the white matter. Neurons and astrocytes occasionally contain round intranuclear inclusion bodies that are approximately 5 um diameter and brightly eosinophilic. Morphologically-similar, intracytoplasmic inclusions are rare. Perivascular cuffing throughout the grey and white matter is characterized by mild to marked expansion of Virchow-Robbins space by small numbers of densely-packed lymphocytes and fewer plasma cells.

Contributor's Morphological Diagnosis:

Brain: Severe multifocal demyelination with lymphoplasmacytic perivascular encephalitis, gliosis and neuronal and astrocytic, intranuclear and intracytoplasmic inclusion bodies.

Contributor's Comment:

This case highlights an excellent example of canine distemper virus infection in the brain of a dog. Astrocytes and neurons contain both intracytoplasmic and intranuclear viral inclusion bodies, which are characteristic of Canine Distemper Virus (CDV) and other Paramyxoviruses including Newcastle Disease Virus, Measles Virus and Rinderpest Virus. The first supplementary image illustrates immunoreactivity for CDV within a neuron. The second supplementary image highlights demyelination and status spongiosis of the white matter, which has been proposed to be consequent to the direct effect of the virus on oligodendrocytes. Interestingly, there is no ultrastructural evidence of viral infection of oligodendrocytes.[5] However, studies over the past decade have suggested that an axonopathy precedes demyelination, therefore promoting speculation that CDV encephalopathy is not a primary demyelinating disease.[4]

Four distinct presentations of CDV within the central nervous system have been characterized: classic canine distemper, multifocal distemper encephalomyelitis in mature dogs, old dog encephalitis and post-vaccinal canine distemper encephalitis.

Despite discrepancies in clinical presentation, initial disease pathogenesis remains similar across all four presentations. Upon inhalation, viral particles gain access to macrophages and epithelial cells through the signaling lymphocyte activation molecule (SLAM) and nectin-4 receptor, respectively. The virus travels within these infected leukocytes to regional lymph nodes and the tonsils, where viral replication occurs over the

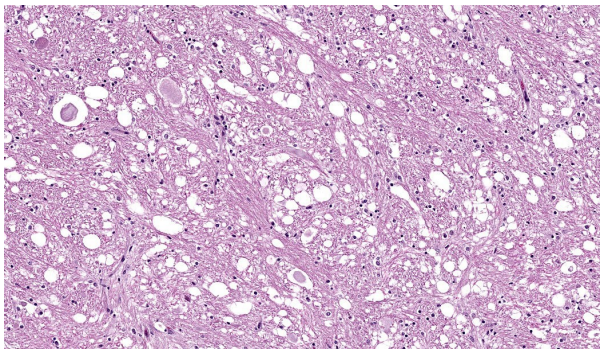

Figure 4-3. Cerebrum, dog: In areas of thalamic spongiosis, there is marked dilation of myelin sheaths with spheroid formation. (HE, 273X)

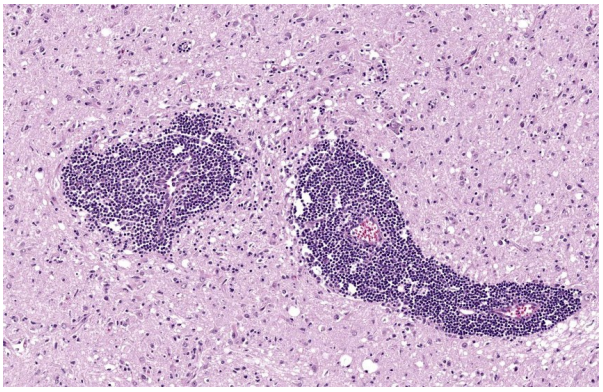

Figure 4-4. Cerebrum, dog: There is marked expansion of Virchow-Robin's spaces within the thalamus by numerous lymphocytes and plasma cells. (HE, 212X)

first twenty four hours of infection. Cell-associated viremia follows and the virus spreads to all lymphoid tissues and blood lymphocytes by five days post-infection. Viral infection of lymphoid tissues and lymphocytes results in lymphocytolysis and leukopenia, which ultimately leads to immunosuppression. Following initiation of immunosuppression, the clinical course depends largely on the host immune response, namely whether there is adequate, delayed/ intermediate or a failure of humoral/cellular immunity.

Within the presented case, the patient's advanced age and reported history of canine distemper are most consistent with old dog encephalitis (ODE). Old dog encephalitis is rarely reported and therefore its pathogenesis remains poorly understood. Nonetheless, ODE is believed to develop within immunocompetent individuals with a subclinical, persistent infection. A replication-defective virus is suspected to persist within neurons of the central nervous system.[2] Notably, a recent study provided evidence that non-cytolytic, cell-to-cell viral transmission occurs within astrocytes through a third receptor that is independent of SLAM and nectin-4.[1]

Although ODE appears to be a chronic disease, clinical presentation may be acute with sudden onset of neurologic abnormalities. This form of the canine distemper progresses over several months until the patient becomes comatose and eventually dies. At the time of this patient's workup, no effective treatment or preventative for ODE had been identified.

Contributing Institution:

University of California, Davis Veterinary Medical Teaching Hospital
https://www.vetmed.ucdavis.edu/hospital

JPC Morphologic Diagnosis:

Cerebrum: Demyelination, multifocal to coalescing, severe, with gliosis, perivascular cuffing, and neuronal and glial intranuclear and intracytoplasmic viral inclusions.

JPC Comment:

Wrapping up this conference was a stunning case of canine morbillivirus with readily identifiable viral inclusions. Canine distemper virus is a top infectious cause of demyelinating injury in dogs. This is due to direct infection and destruction of glial cells, such

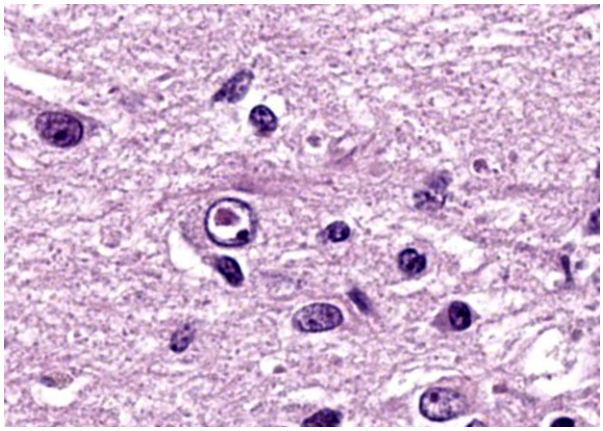

Figure 4-5. Cerebrum, dog: Rare thalamic neurons contain large 4-5um eosinophilic intranuclear viral inclusions. (HE, 565X)

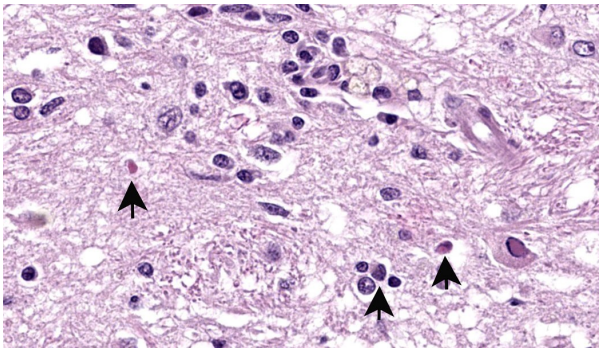

Figure 4-6. Cerebrum, dog: Rare thalamic glial cells contain smaller 2-3um eosinophilic intracytoplasmic viral inclusions (arrows). A neuron with an intranuclear inclusion is at right. (HE, 565X)

as oligodendrocytes (primary myelinating cell of the CNS), astrocytes, and microglia.[3,5] CDV can also infect neurons, including Purkinje's cells and granular cells.[3] The cerebellum is consistently affected in cases of CDV, with demyelinating lesions in the cerebellar white matter. Other common sites for similar lesions include the periventricular white matter (especially around the 4th ventricle) and the optic pathways.[3] Occasionally, the white matter of the spinal cord may be involved. The Pesavento Lab also performed IHC on this case and was able to readily demonstrate the virus within glial cells and neurons in this case.

In acute and subacute cases of CDV, astrocytes and oligodendrocytes are infected in the early demyelinating phase. This manifests predominantly as vacuolation and/or dilation of myelin sheaths, demyelination, and axonal swelling (spheroids), +/- digestion chambers. The distribution is frequently multifocal but is usually concentrated in the caudal brainstem and cerebellum. The viral inclusion bodies of CDV (known as "Lentz bodies") can be seen either in the nucleus or cytoplasm of infected cells both within the brain and in other tissues.[3,5]

"Old dog encephalitis" (ODE) is a controversial condition. The paper that describes this condition had eight dogs total in the study, with one being experimentally infected.[2] ODE is a disease of neurons and grey matter, especially in the cerebral cortex and thalamus, which contrasts starkly with the caudal brain predilection of acute/subacute CDV infection.[2] Although viral antigen was densely expressed in neurons in the ODE paper, the demyelinating component of this disease was less pronounced.[2] In cases of ODE, the cerebellum and caudal brainstem are comparatively spared.[2] As such, there is still room for interpretation on the cause of ODE and the correlation, or lack thereof, with replication-deficient CDV infection.

CDV manifests in a variety of other ways outside of the CNS due to remarkable pleocellular tropism. These include pustular dermatitis and nasodigital hyperkeratosis/ parakeratosis (also known as "hard pad disease"), enamel hypoplasia/dysplasia, ocular manifestations, myocardial necrosis, and metaphyseal osteosclerosis. Metaphyseal osteosclerosis occurs as CDV infects osteoclasts directly, causing a growth retardation lattice (also known as a "double line") within the bony trabeculae due to lack of trabecular resorption during bone maturation. Currently, it is unknown which tissue sample is the most sensitive for testing due to CDV's incredibly broad cellular tropism.

Another historical ruleout for spongiosis in the white matter of a dog that was mentioned by one participant (old enough to remember when it was banned by the FDA is hexachlorophene, which also results in a similar spongiotic and demyelinating injury).

References:

1. Alves L, Khosravi M, Avila M, et al. SLAM- and nectin-4-independent non-

cytolytic spread of canine distemper virus in astrocytes. *Journal of Virology.* 2015;89:5724-5733.

2. Axthelm M, Krakowka D. Experimental old dog encephalitis (ODE) in a gnotobiotic dog. *Veterinary Pathology.* 1998;35:527-534.

3. Carvalho OV, Botelho CV, Ferreira CG, Scherer PO, Soares-Martins JA, Almeida MR, Silva Júnior A. Immunopathogenic and neurological mechanisms of canine distemper virus. Adv Virol. 2012;2012:163860.

4. Lempp C, Spitzbath I, Puff C, et al. New aspects of the pathogenesis of canine distemper leukoencephalitis. *Viruses.* 2014;6:571-601.

5. Vandevelde M, Zurbriggen A. The neurobiology of canine distemper virus. *Veterinary Microbiology.* 1995;44:271-280.